OPTOELECTRONICS AND ADVANCED MATERIALS – RAPID COMMUNICATIONS Vol. 15, No. 11-12, November-December 2021, p. 578-585

Target's laser radiation energy calculation and detection performance in laser-screen

HANSHAN LI*, HUI GUAN
School of Electronic and Information Engineering, Xi'an Technological University, Xi'an, 710021, China

The sky-screen is a kind of sensor for detecting flying projectile. Due to the uncertainty of the test environment, the traditional sky-screen cannot work stably. Especially in the low environmental illumination, the detection ability of the traditional sky-screen is too low to meet the detection requirements of the projectile in the weapon testing range. In order to improve the detection ability of traditional sky-screen in the low environmental illumination, based on the detection principle of the traditional sky-screen, this paper designs a fan-shaped laser source with a certain thickness by using high-power laser, the high-power laser is located in the traditional sky-screen, meantime, make the fan-shaped laser area coincide with the detection area of the traditional sky-screen, the test system formed is called laser-screen. When the target passes through the detection area of laser-screen, we establish a calculation model of laser reflected energy and target radiation flux, and derive the signal-to-noise ratio function of the target detected by the laser-screen according to this. Through calculation and experiment, we obtain the conclusion that when the environmental illumination is less than 1800Lx, the signal-to-noise ratio of the laser-screen can reach more than 4.5, while the signal-to-noise ratio of the traditional sky-screen is less than 1.5, the results show that the detection ability of the new designed laser-screen is significantly better than that of the traditional sky-screen.

(Received June 18, 2021; accepted November 24, 2021)

Keywords: Laser-screen, Reflected laser, Detection screen, Target, Signal-to-noise ratio

1. Introduction

The sky-screen is a kind of sensor for detecting projectile information in the weapon testing range, the measurement system of four, six and seven sky-screens were formed by using multiple sky-screens, combined with the test requirements, we use the corresponding measurement system to measure the relevant parameters of the projectile. For the multiple screens measurement system, the detection ability and detection stability of the single sky-screen are the core factors of the measurement system, these factors restrict the performance of the multiple screens measurement system. The traditional sky-screen mainly adopts the photoelectric detector in the natural light band. When the traditional sky-screen is tested in the weapon testing range, due to the large change of the environmental illumination in a whole day, and the illumination range is from 500Lx to 200000Lx, the results are that the inherent noise of the detection circuit is changed with the change of the environmental illumination, and affects the signal-to-noise ratio (SNR) of the traditional sky-screen [1-2]. Based on this, the detection stability of the multiple screens measurement system is poor. With the development of intelligent weapons, higher test requirements are put forward for the measurement system. We need to develop a new measurement system that can test stably all-weather and obtain scientific test data to speed up the research and development of weapons. In order to meet the test requirements of the current weapon test range, Yanan Tian et al. proposed a measurement method of the response time consistency for sky-screens vertical target, which improved the velocity measurement accuracy of test equipment [3]. Yan Lou et al. studied Hopfield auto-associative neural network to identify and eliminate the typical interference, the purpose is to improve the test accuracy and reliability of sky screen [4]. Hui Tian et al. proposed a method to measure the projectile flight parameters of variable speed parabolic ballistic, which improved the measurement accuracy of the sky-screen for variable speed flying target parameters [5]. Rui Chen et al. studied the calibration method of detection screen plane of sky-screen, the purpose is to reduce the test error caused by human factors [6,7]. In view of the high electromagnetic interference of the sky-screen, Yugui Song et al. proposed a new type of velocity measurement coil sensor with differential structure, which improved the stability of the sky screen target [8]. Although these improvement measures effectively improve the performance of the sky-screen, for the sky-screen with natural light as the detection background light source, it is still affected by the environment and can't work around the clock.

In this paper, a high-power laser is used to form an active light source, which is a fan-shaped area with a certain thickness. The fan-shaped area is coincident with the detection area of the traditional sky-screen, and an active laser detection area is designed. When the projectile passes through the laser detection area, the photoelectric detector not only senses the changing luminous flux caused by the target passing through the detection area in a short time, but also senses the laser energy reflected from the target's surface into the photosensitive surface.

Because the detection distance of the test system is relatively close, the attenuation of laser energy caused by long-distance transmission can be ignored, and the emission power of laser is very little affected by environmental illumination. Therefore, the laser-screen formed by introducing laser into traditional sky-screen can be tested all-weather. In order to scientifically analyze the detection ability of laser-screen, we analyse the energy distribution of emitting laser fan-shaped light source, the energy distribution of target reflection and the influence of laser on detection circuit, and establish the calculation model of SNR of the laser-screen. At this same time, the multiple array laser-screen test system with certain spatial geometric relationship is composed of multiple laser-screens, so as to improve and stabilize the test performance of the multiple array laser-screen test system and meet the test requirements of the weapon test range.

2. The detection principle of laser-screen and the energy distribute of laser emission

Laser-screen is mainly composed of the laser emitting module, the laser receiving module and signal processing circuit, the detection diagram of laser-screen is shown in Fig. 1.

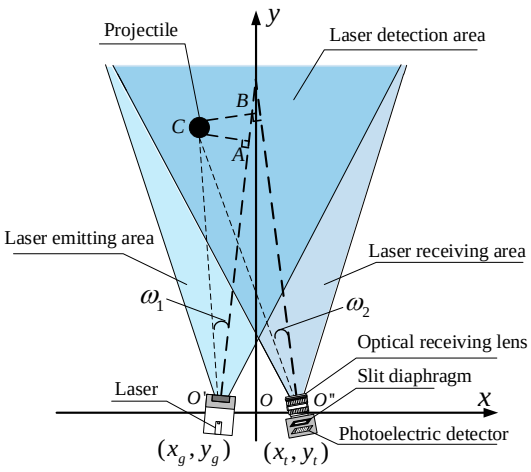

Fig. 1. The detection principle of laser-screen

In the Fig. 1, the laser emitting module is composed of a emitting laser with high-power and a cylindrical lens with beam expanding function. The laser can form the fan-shaped area with a certain thickness through the cylindrical lens. The laser receiving module consists of an optical receiving lens, a slit diaphragm and a photoelectric detector. The fan-shaped receiving area of the laser receiving module is formed by optical receiving lens and slit diaphragm in the air, and whose field of view is consistent with that of the detection area. The projectile through the laser-screen can reflect part of the laser energy to the photoelectric detector, which cause the luminous flux of the photoelectric detector changes, meanwhile, the projectile passing through the laser-screen also causes the change of the luminous flux of the photoelectric detector, and then the electrical signal is output and processed by the signal processing circuit. The size of the output signal represents the detection performance of the system, which is mainly affected by the target radiation characteristics and target reflection characteristics [9,10]. The sources causing the changes of these characteristics of the target includes laser, natural light, light reflected by environment and so on. Therefore, it is necessary to establish the calculation model of luminous flux received by photoelectric detector of the laser-screen.

As shown in Fig. 1, a two-dimensional coordinate system is established with the midpoint between the laser emitting module and the laser receiving module as the origin o. Suppose that the coordinate of the projectile passing through the laser screen is (x_m, y_m); the coordinate of the laser emitting module is (x_g, y_g); and the coordinate of the laser receiving module is (x_t, y_t). o' is the the optical axis center point of the laser emitting module, o'' is the optical axis center point of the laser receiving module. ω_1 is the angle between the projectile and the center line of laser emitting area; ω_2 is the angle between the projectile and the center line of the laser receiving area. Line *AC* is perpendicular to the optical axis of the laser emitting area, the linear equation of the line $o'A$ in the *oxy* coordinate system is $y = x\tan\beta_1 + b_1$, and $\tan\beta_1$ represents the slope of the line $o'A$, b_1 is a constant, and which is related to the distance between the laser emitting module and the origin o of the *oxy* coordinate system. The linear equation of line *AC* in *oxy* coordinate system is $y = -\dfrac{x}{\tan\beta_1} + b_2$, and $-\dfrac{1}{\tan\beta_1}$ represents the slope of the line *AC*, and b_2 is a constant. Similarly, Line *BC* is perpendicular to the optical axis of the laser receiving area, and the linear equation of the line $o''B$ in the *oxy* coordinate system is $y = x\tan\beta_2 + b_3$, and $\tan\beta_2$ represents the slope of the line $o''B$, b_3 is a constant, which is related to the distance between the laser receiving module and the origin o of the *oxy* coordinate system. The linear equation of line *BC* in *oxy* coordinate system is $y = -\dfrac{x}{\tan\beta_2} + b_4$, and $-\dfrac{1}{\tan\beta_2}$ represents the slope of the line *BC* and b_4 is a constant. Considering the attenuation characteristics of aerosol particles in air to laser energy [11-13], the laser power distribution at different positions in the laser-screen is given:

$$P_{m0} = P_0 e^{-\varepsilon H_g} \cos\omega_1 \tag{1}$$

Here, P_0 is the laser emission power; ε is the attenuation coefficient of aerosol particles in air.

We assume that H_g is the distance between the position and the optical axis center point o' of the laser emitting module, and which is line $o'C$ in the Fig. 1. H_t is the distance between the position and the optical axis center point o'' of the laser receiving module, and which is line $o''C$ in the Fig. 1. Combined with the relationship of multiple linear equations given in Fig. 1, H_g and H_t are calculated by formulas (2) and (3) respectively .

$$H_g = \sqrt{\left(\frac{y_m + \frac{x_m}{\tan\beta_1} - b_1}{\tan\beta_1 + \frac{1}{\tan\beta_1}} - x_g\right)^2 + \left(\frac{\tan\beta_1\left(y_m + \frac{x_m}{\tan\beta_1} - b_1\right)}{\tan\beta_1 + \frac{1}{\tan\beta_1}} + b_1 - y_g\right)^2} \tag{2}$$

$$H_t = \sqrt{\left(\frac{y_m + \frac{x_m}{\tan\beta_2} - b_3}{\tan\beta_2 + \frac{1}{\tan\beta_2}} - x_t\right)^2 + \left(\frac{\tan\beta_2\left(y_m + \frac{x_m}{\tan\beta_2} - b_3\right)}{\tan\beta_2 + \frac{1}{\tan\beta_2}} + b_3 - y_t\right)^2} \tag{3}$$

The laser energy of the laser emitting area follows the Gaussian distribution [14-16], therefore, in the laser detection area of the laser-screen, the laser energy centered on the laser optical axis is the highest. With the extension to both sides of the laser detection area, the laser energy decreases gradually, the laser energy at different positions of the laser detection area is as follows:

$$P_m = P_0 \cdot \cos\omega_1 \cdot e^{-\varepsilon H_g} \times e^{-\frac{\left(R_{sy}\tan\left(\arctan\frac{y_m - y_g}{x_m - x_g} - \beta_1\right)/\tan(\alpha_1/2)\right)^2}{2}} \tag{4}$$

Here, R_{sy} is the waist radius of Gaussian distribution; α_1 is the divergence angle of laser detection area.

The projectile is non-lambert body, the ordinary reflection coefficient is not accurately describe the laser reflection characteristic, and the calculated luminous flux induced by the photoelectric detector is not accurate enough [17]. Therefore, according to the bidirectional reflection distribution function, combined with the inverse relationship between the angle between the laser reflected by the projectile's surface and the normal of the projectile's surface and the power reflected by the projectile's surface, the calculation model of the laser power reflected by the projectile's surface is established.

$$\begin{aligned} P_f &= P_m \rho(\gamma_m) \\ &= P_m \frac{k_b k_\gamma^2 \cos\gamma_\alpha \ln(1+\cos^2\gamma_m)}{\pi \ln 2[1+(k_\gamma^2-1)\cos\gamma_\alpha]} \\ &\quad \times \exp[-|\gamma_b|(1-\cos\gamma_\gamma)^{\gamma_d}] + \frac{k_d(\cos\gamma_m)^{2f_d}}{\pi} \end{aligned} \tag{5}$$

Here, k_b , k_r , k_d , γ_b , f_d is the undetermined coefficient of the bidirectional reflection function; The part of the target's surface illuminated by the laser is called plane A, which is divided into a plurality of micro planes with equal area, and A' is the micro plane. γ_α is the angle between the normal of the micro plane A' and the normal of the plane A; γ_r is the incident angle of the plane coordinate system *xoy* on the micro plane A', γ_m is the angle between the target and the laser optical axis.

The laser power reflected by the projectile's surface is not only related to the reflection area of the target, but also related to the duration time that the projectile passes through the laser detection area, and the relationship between the projectile's length and the thickness of the laser detection area [18]. So, the laser power reflected by the projectile passing through the laser detection area can be divided into two cases, one is that the projectile's length is greater than the thickness of laser detection area, and the other is that the projectile's length is less than the thickness of laser detection area. When the projectile's length is larger than the thickness of the laser detection area, the effective area of the projectile reflecting the laser is the product of the projectile's diameter and the thickness of the laser detection area. On the contrary, the effective area of the projectile reflecting the laser is the product of the diameter and the length of the projectile. So, the calculation model of luminous flux of laser reflected by projectile's surface incident on photoelectric detector is as follows:

$$\Phi_{fz} = \begin{cases} \dfrac{4d\varpi H_g^{\,2} P_m \rho(\gamma_m)\tan^2\alpha_2}{v_m} & l > L_g \\ \dfrac{2d\varpi l H_g P_m \rho(\gamma_m)\tan\alpha_2}{v_m} & l > L_g \end{cases} \tag{6}$$

Here, d is the diameter of projectile; l is the length of projectile; ϖ is the conversion coefficient of laser's power and luminous flux; α_2 is the divergence angle of the laser detection area, L_g is the thickness of the laser detection area.

After the laser is reflected by the projectile's surface, it passes through the atmosphere and optical receiving lens at a certain distance and reaches the photosensitive surface of the photoelectric detector. At this time, the luminous flux on the photoelectric detector is calculated as follows:

$$\Phi_{fz}=\begin{cases}\dfrac{4\mathrm{d}\varpi\lambda_g H_{\mathrm{t}}{}^2 P_m\rho(\gamma_m)e^{-\varepsilon\sqrt{(y_m-y_t)^2+(x_m-x_t)^2}}\tan^2\alpha_2}{v_m} & l>L_g\\ \dfrac{2\mathrm{d}\varpi l\lambda_g H_t P_m\rho(\gamma_m)e^{-\varepsilon\sqrt{(y_m-y_t)^2+(x_m-x_t)^2}}\tan\alpha_2}{v_m} & l<L_g\end{cases} \tag{7}$$

Here, v_m is the velocity of projectile; λ_g is the transmittance of the optical system to the laser.

The projectile blocks the natural light entering the photosensitive surface of the photoelectric detector that the duration time of the projectile passing through the laser detection area, resulting in the change of luminous flux sensed by the photoelectric detector. According to the influence of the projectile's diameter, the projectile's length, the thickness of laser detection area, the natural illumination and other factors on the luminous flux induced by the photoelectric detector, the calculation function is established by formula (8).

$$\Phi_{tyg}=\begin{cases}\dfrac{2dsf\tau\pi\lambda_z L_0\cos^4(arc\dfrac{y_m-y_t}{x_m-x_t}-\beta_2)\tan\alpha_2}{v_m} & l>L_g\\ \dfrac{2dlf^2\tau\pi\lambda_z L_0\cos^4(arc\dfrac{y_m-y_t}{x_m-x_t}-\beta_2)\tan\alpha_2}{H_{\mathrm{t}}v_m} & l<L_g\end{cases} \tag{8}$$

Here, τ is the vignetting coefficient of the nature light passing through the laser detection area; λ_z is the transmittance of the optical system to natural light; and L_0 is the natural light illumination.

Large dust particles or other similar objects in the natural environment, these objects are irradiated by natural light to form a certain reflection, and are reflected on the projectile's surface and incident on the photosensitive surface of the photoelectric detector, which make a certain contribution to the luminous flux induced by the photoelectric detector [19-21]. Assuming that the reflection coefficient of the background to the natural light is η_{m} and the angle between the reflected light and the projectile's surface is β_{dm}, and the luminous flux of the reflected light of the object in the natural environment incident on the photosensitive surface of the photoelectric detector through the projectile's surface is:

$$\Phi_{dm}=\begin{cases}\dfrac{4\mathrm{d}\lambda_z\eta_m\eta_d H_{\mathrm{g}}{}^2 L_0\cos\beta_{dm}\cos^4(arc\dfrac{y_m-y_t}{x_m-x_t}-\beta_2)\tan^2\alpha_2}{v_m} & l>L_g\\ \dfrac{2\mathrm{d}l\lambda_z\eta_m\eta_d H_{\mathrm{g}} L_0\cos\beta_{dm}\cos^4(arc\dfrac{y_m-y_t}{x_m-x_t}-\beta_2)\tan\alpha_2}{v_m} & l<L_g\end{cases} \tag{9}$$

Here, η_d is the light reflection coefficient of projectile's surface to the object in the natural environment.

3. Calculation of SNR of laser-screen

When there is no projectile passing through the laser detection area, the photoelectric detector mainly senses the incidence of natural light and the backscattering of dust particles in the air. The attenuation of laser by dust particles in the air mainly comes from the absorption and backscattering of dust particles, and the laser backscattered by dust particles enters the photoelectric detector. If the backscattering coefficient of dust particles is large enough, the photoelectric detector will cause false alarm because the induced luminous flux is large and exceeds the threshold set by the laser-screen. Therefore, considering the contribution of backscattering of dust particles in the air, the mathematical model of ambient background luminous flux received by the photoelectric detector is:

$$\Phi_B=\frac{2H_g K^2\tan\alpha_2(\lambda_z E_0+\lambda_g\varpi G_{ss}P_0)}{v_m} \tag{10}$$

Here, G_{SS} is the backscattering coefficient of the dust particles to the laser; K is the side length of the photoelectric detector.

Based on the detection principle of the photoelectric detector, when the luminous flux received by the photosensitive surface of the photoelectric detector changes, the photoelectric detector outputs an electrical signal that can be analyzed intuitively through the photoelectric conversion circuit. When there is no projectile passing through the laser detection area, the voltage signal calculation model of the photoelectric detector output noise signal is as follows:

$$V_B=\frac{2\vartheta H_g K^2\tan\alpha_2(\lambda_z E_0+\lambda_g\varpi G_{ss}P_0)uKR}{v_m} \tag{11}$$

Here, ϑ is the average coefficient of air particle density in a certain period of time; u,K,R are the magnification, photoelectric conversion coefficient and equivalent resistance of the photoelectric detector respectively.

When the projectile passes through the laser detection area, the photosensitive surface of photoelectric detector receives the laser energy reflected from the photosensitive surface of photoelectric detector, the reflection characteristics of the environmental background and the change of luminous flux caused by the projectile blocking natural light, the calculation model of the projectile voltage signal output by the laser-screen is as follows:

$$V_M=(\Phi_{fz}-\Phi_{tyg}+\Phi_{dm})uKR \tag{12}$$

Based on the definition of signal-to-noise ratio of the photoelectric detection system, combined with the calculation model of projectile signal and background noise signal, the calculation model of signal-to-noise ratio of laser-screen is established by formula (13).

$$SNR = \frac{v_m(\Phi_{fz} - \Phi_{tyg} + \Phi_{dm})}{2\vartheta H_g K^2 \tan\alpha_3(\lambda_z E_0 + \lambda_g \varpi G_{ss} P_0)} \tag{13}$$

4. Calculation and experiment

4.1. Calculation and analysis

Assuming that the laser emission power of the laser-screen can be adjusted, the range is 0W to 120W. The focal range of the laser receiving optical lens is 35 mm-100 mm, the field of the detection light curtain of the laser screen reaches 54° by adjusting the focal length of the laser receiving optical lens. The width of the silt aperture is 0.2 mm-0.6 mm, and the purpose is to adjust the noise voltage of the test system to the most suitable state under different environmental illuminances. According to the laser power distribution model and laser reflection power model of the laser-screen, the laser power distribution diagram under different position conditions is given, as shown in Fig. 2, and the laser reflection power distribution diagram in the effective detection area is shown, as shown in Fig. 3.

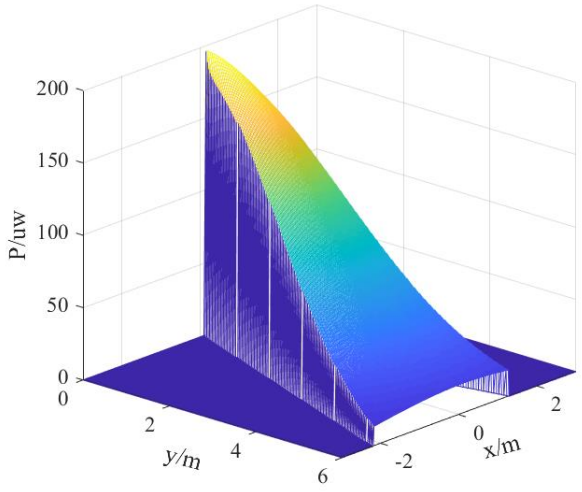

Fig. 2. The laser power distribution diagram under different position conditions of laser-screen (color online)

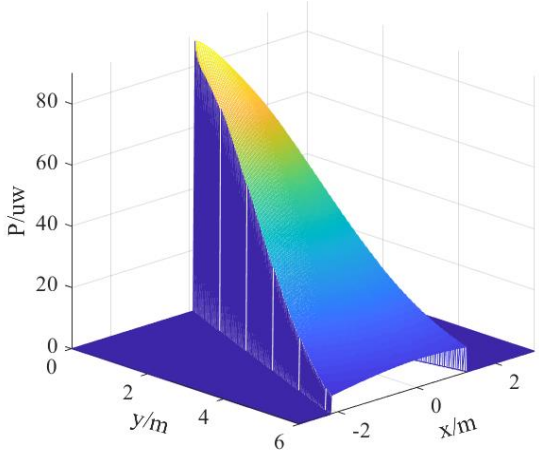

Fig. 3. The laser reflection power distribution diagram in the effective detection area of laser-screen (color online)

As can be seen from Figs. 2 and 3, since the laser beam energy is scattered and absorbed by dust particles when the laser beam propagates in the air, the laser power and laser power reflected by the projectile's surface gradually decrease with the increase of detection distance. At the same time, the laser power is Gaussian distribution when the projectile passes the different detection field at the same detection distance, and the laser reflection power reflected into the photoelectric detector is also Gaussian distribution, that is, the laser reflection power at the center of the optical axis of the detection field is the strongest, and the laser reflection power at the edge of the detection field is the weakest. Based on the setting of the system and the principle of optical detection, when the detection distance is about 0.705 m, it is considered that the length of the projectile is close to the thickness of the detection screen. Therefore, when the detection distance is less than 0.705 m, the attenuation trend of laser reflection power is not significant. Once the detection distance is greater than 0.705 m, the attenuation trend of laser reflected power is obvious.

Fig. 4 shows the SNR curve of the system when the laser reflected power changes.

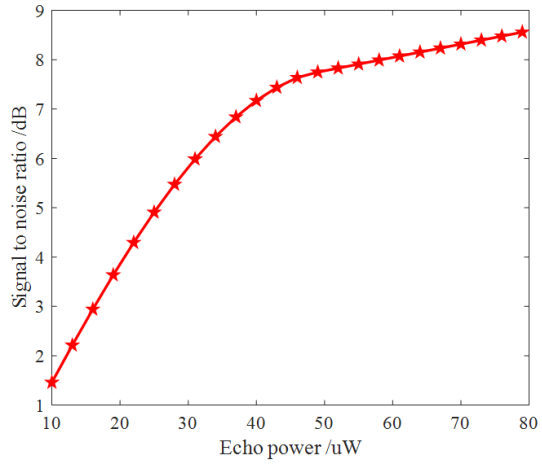

Fig. 4. The SNR curve of the system when the laser reflected power changes

It can be seen from Fig. 4 that, with the laser emission power increases, the laser echo power also increases, and the SNR of system also increases. At the same time, due to the increase of the laser emission power, the system noise has increased to a certain extent, which makes the growth trend of the system signal-to-noise ratio gradually slow.

4.2. Experiment and analysis

In order to verify the effectiveness of the SNR model established in this paper, we carried out the corresponding experiments. For the laser-screen, the laser emission power is adjusted to 40W, the frequency of the laser emission system is 3kHz, by adjusting the focal length of the laser receiving optical lens so that its field of view angle is 32 °, the aperture of the optical lens is 1:1.8, the transmittance of the optical lens to the laser is 0.92 and the transmittance to the sunlight is 0.85. The divergence angle of the laser emitting module is consistent with the field angle of view of the laser receiving module, both of which are 32 °. The included angle between the laser emitting module and the horizontal ground is 85 °, the included angle between the laser receiving module and the horizontal ground is 95 °. The distance between the laser receiving module and the laser emitting module is 0.2 m [22]. The sensitive surface of the photoelectric detector is $2mm \times 2mm$. The site layout is as follows: the sky screen, laser-screen and wooden target are placed in the trajectory, the detection screens of the two test systems are completely parallel, and the centers of the detection screens coincide. The sky screen is closest to the firing position of the muzzle. The laser-screen is about 1m away from the sky-screen. The wooden target is placed 2m away from the sky-screen to record the position of the projectile passing through the detection screen. The diameter of the projectile used for shooting is 7.62 mm. In the first round of test, the illumination of the test environment is 1800Lx, the weapon firing position is in the center of the detection field of view, and the detection distance range is 1 m-5 m. Table 1 records the projectile signals and noise signals output by the laser-screen under different detection distances, among, the saturation value of the projectile signals output by the laser-screen and the sky screen are both 5000 mV, V_J is the projectile signal and V_{JZ} is the noise signal.

According to Table 1, when the background illumination is 1.8×10^3 cd/m^2, the average background noise of the laser-screen is 540 mV, the SNR is about 5.79. Although the average background noise of the sky-screen is slightly less than laser-screen and the noise of the sky-screen is about 365 mV. Because the amplitude of the projectile signal output by the sky-screen is relatively small, the threshold SNR of 1.5 set by the sky-screen cannot be met, and the sky-screen cannot detect the projectile under the test conditions. The detection performance of the laser-screen is significantly better than the sky-screen under the same test condition. At the same time, the projectile signal of the laser-screen decreases with the increasing detection distance, which is in line with the detection law of the photoelectric detection system, and is consistent with the calculation model of formula (12).

Table 1. The projectile signals and noise signals output by the laser-screen under different detection distances

No.	y/m	x/m	V_J/mV	V_{JZ}/mV
1	1.08	0.16	4992	556
2	1.9	-0.12	4720	532
3	2.21	0.14	4245	536
4	2.45	-0.15	4186	569
5	2.91	0.11	3254	521
6	3.32	-0.08	2746	533
7	3.65	0.38	2344	551
8	4.22	-0.17	1847	514
9	4.55	0.18	1743	549
10	5.11	0.03	1315	538

Fig. 5 shows the trend of the projectile signal distribution of the two surface roughness of projectile under different laser emission power conditions. The surface roughnesses of projectile are 0.1 and 0.05 respectively, the diameters of projectiles are both 7.62 mm. As the laser emission power increases, the projectile signal output of the laser-screen also increases, and the smaller the projectile surface roughness, the greater the amplitude of the projectile signal output by the laser-screen.

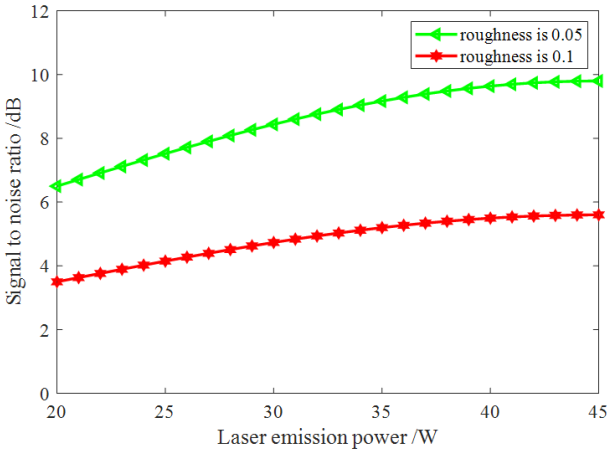

Fig. 5. The trend of the projectile signal distribution of the two surface roughness of projectile under different laser emission power conditions (color online)

In the second round of test, the weapon firing position is still in the center of the detection field of view, and the detection distance is about 2.5 m. Under the same laser emission power, shoot projectiles with different surface roughness respectively, adjust the laser emission power, and record the SNR test results of the laser-screen under

the different surface roughnesses of projectile and different laser emission powers, as shown in Table 2, among, SNR_1 represents the SNR of the laser-screen when the surface roughness of the projectile is 0.05, and SNR_2 represents the SNR of the laser-screen when the surface roughness of the projectile is 0.1. The test results in Table 2 are completely consistent with the variation law in Fig. 5.

Table 2. SNR test results of the laser-screen under the different surface roughnesses of projectile and different laser emission powers

No.	P_0 / W	SNR_1 / dB	SNR_2 / dB
1	20	6.04	3.6
2	22	6.28	3.92
3	25	6.53	4.14
4	27	7.03	4.45
5	30	7.29	4.73
6	32	7.45	4.84
7	35	7.91	4.91
8	37	8.01	5.35
9	40	8.25	5.37
10	45	8.37	5.56

The noise of laser-screen is related to natural light, laser emission power and dust particle density in the air. Fig. 6 shows that the relationships curve between the SNR and background illumination under different dust particle density. With the increase of background illumination, the SNR of the laser-screen decreases gradually, the SNR of the laser-screen under the condition of high dust particle density is significantly lower than that under the condition of low dust particle density.

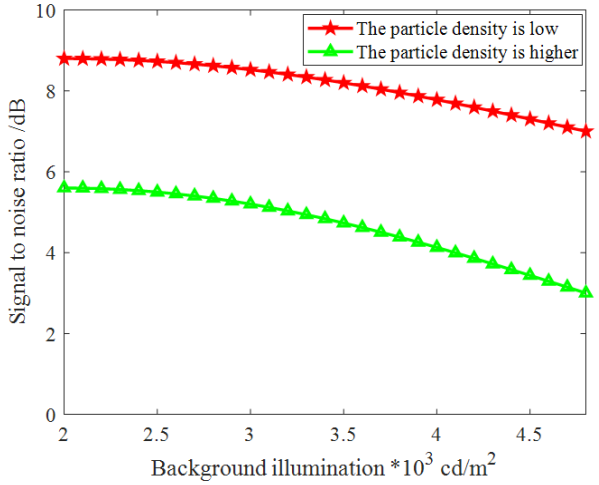

Fig. 6. The relationships curve between the SNR and background illumination under different dust particle density (color online)

The data in Table 3 are the target signal amplitude peak value and noise mean value under the condition of 2.3 m height and two kinds of air particle density coefficient and different background illuminations. V_{min} is the SNR of the target signal under the condition of small particle density, and V_{max} is the SNR of the target signal under the condition of large particle density. The distribution of SNR of target signal is in accordance with the trend and data shown in simulation Fig. 6, which proves that the air particles and background illuminance have an impact on the SNR of target signal.

In the third round of tests, two test environments with different dust particle density were artificially simulated. The weapon was still firing at the center of the detection field of view and the detection distance is approximately 2.3 m. Record the SNR of the laser-screen under different dust particle density, as shown in Table 3, among, SNR_{min} indicates the SNR of the laser-screen under the small dust particle density and the SNR_{max} indicates SNR of the laser-screen under the large dust particle density.

Table 3. The SNR of the laser-screen under different dust particle density

No.	Background illumination / 10^3 cd / m^2	SNR_{min} / dB	SNR_{max} / dB
1	2.5	8.76	5.53
2	3	8.51	5.28
3	3.5	8.28	4.84
4	4	7.87	4.26
5	4.5	7.42	3.58

The test data in Table 3 are consistent with the results in Fig. 6, the results show that the effect of dust particle density and background illumination affect the SNR of the laser-screen.

5. Conclusions

Based on the detection principle of the laser-screen and considering the radiation characteristics and laser reflection characteristics of the projectile's surface when the projectile passes through the detection screen, we establish the calculation model of the luminous flux induced by the photoelectric detector of the laser-screen, and derive the calculation model of the SNR of the laser-screen. Through calculation and analysis, the influence of laser emission power on the SNR of laser-screen is explained; then, the tests of different detection distances, different laser emission powers and different environmental illumination conditions are carried out to verify the feasibility of the SNR calculation model of the laser-screen established in this paper, which provides a new idea for improving the detection ability of photoelectric detection system in complex environment.

Acknowledgment

This work has been supported by Project of the National Natural Science Foundation of China (No.62073256, 61773305), in part by the Key Science and Technology Program of Shaanxi Province (No.2020GY-125) and Xi'an Science and Technology Innovation Talent Service Enterprise Project (No.2020KJRC0041).

References

[1] Hanshan Li, Xiaoqian Zhang, Xuewei Zhang, Liping Lu, Measurement **177**, 109281 (2021).
[2] Liping Lu, Xiaoqian Zhang, Hui Guan, Lei Yao, Journal of Ordnance Equipment Engineering **42**(8), 164 (2021).
[3] Yanan Tian, Hui Tian, Yun Yuan, Journal of Applied Optics **40**(3), 483 (2019).
[4] Yan Lou, Yiwu Zhao, Yugui Song, Weifang Zhang, Acta Armamentarii **35**(10), 1587 (2014).
[5] Hui Tian, Jinping Ni, Mingxing Jiao, Chinese Journal of Scientific Instrument **37**(1), 67 (2016).
[6] Rui Chen, Jinping Ni, Optik **155**, 276 (2018).
[7] Liang Zhao, Zhaoba Wang, Youxing Chen, Guodong Chen, Journal of Projectiles, Rockets, Missiles and Guidance **31**(6), 213 (2011).
[8] Yugui Song, Yong Wang, Bin Xin, Baisheng Kai, Tairan Zhang, Chinese Journal of Scientific Instrument **41**(12), 95 (2020).
[9] Qijie Tian, Zhou Li, Songtao Chang, Fengyun He, Yanfeng Qiao, Acta Optica Sinica **37**(10), 191 (2017).
[10] Lihua Cao, Chunming Wan, Yunfeng Zhang, Ning Li, Journal of Infrared and Millimeter Waves **34**(4), 460 (2015).
[11] Shanshan Zhang, Brandon Lane, Kevin Chou, Measurement Science and Technology **32**(5), 055007 (2021).
[12] B. Muralikrishnan, Measurement Science and Technology **32**(7), 072001 (2021).
[13] Peng Chen, Jiguang Zhao, Yishuo Song, Shen Wang, Infrared and Laser Engineering **49**(6), 187 (2020).
[14] He Yan, Qifeng Zhao, Min Xie, Xiaoling Li, Acta Optica Sinica **41**(5), 97 (2021).
[15] Qian Yi, Haoyu Zhong, Long Liu, Wenlong Liu, Bing Yi, Chinese Journal of Lasers **47**(11), 154 (2020).
[16] Xiaona Wang, Yishu Zhang, Dexin Hou, Shuliang Ye, Infrared and Laser Engineering **49**(7), 152 (2020).
[17] Jundong Fu, Qing Chen, Yunxia Qiu, Cong Ye, Laser and Optoelectronics Progress **56**(11), 190 (2019).
[18] Xiaoqian Zhang, Hanshan Li, Shanshan Zhang, Microwave and Optical Technology Letters **63**(12), 3092 (2021).
[19] Zhiguo Liu, Xiong Qiu, Shicheng Wang, Zhimin Wang, Chinese Journal of Lasers **46**(11), 9 (2019).
[20] Peng Chen, Jiguang Zhao, Yiming Zhang, Yishuo Song, Bo Zhu, Laser Journal **41**(10), 29 (2020).
[21] Hongguang Ren, Haojun Zhang, Yukai Sun, Yunwen Zhang, Infrared and Laser Engineering **49**(4), 29 (2020).
[22] Xiaoqian Zhang, Hanshan Li, Jianjian Cao, Applied Optics **60**(24), 7437 (2021).

*Corresponding author: lihanshan269@163.com